Conference Paper

Torque-speed characteristics for electrically powered rim driven fans and thrust comparison with a small conventional fan jet engine

Bolam, R.C., Roque, J.P.C., Vagapov, Y. and Day, R.J.

This is a paper presented at the 57th IEEE International Universities Power Engineering Conference UPEC-2022, Istanbul, Turkey and is available at
https://ieeexplore.ieee.org/abstract/document/9917918?casa_token=z2z0T7r0RwIAAAAA:tseAIMza1_r55R8lZGqYJSCX6nYzFpve-20YH-93MqIly-QzBcjpEgixMM7mIHrVulZoidGEKh4A-A

Recommended citation:

Bolam, R.C., Roque, J.P.C., Vagapov, Y. and Day, R.J. (2022), 'Torque-speed characteristics for electrically powered rim driven fans and thrust comparison with a small conventional fan jet engine', in: Proc. 57th IEEE International Universities Power Engineering Conference UPEC-2022, Istanbul, Turkey, 30 Aug. - 2 Sept. 2022, pp. 1-5. doi: 10.1109/UPEC55022.2022.9917918

Torque-Speed Characteristics for Electrically Powered Rim Driven Fans and Thrust Comparison with a Small Conventional Fan Jet Engine

Robert Cameron Bolam
Faculty of Art, Science and Technology
Glyndwr University
Wrexham, UK

Jhon Paul C. Roque
Faculty of Art, Science and Technology
Glyndwr University
Wrexham, UK

Yuriy Vagapov
Faculty of Art, Science and Technology
Glyndwr University
Wrexham, UK

Richard J. Day
Faculty of Art, Science and Technology
Glyndwr University
Wrexham, UK

***Abstract*—The aim of this paper is to provide a method of estimating torque versus speed characteristics of single and dual-stage electrically powered Rim Driven Fans which are intended for aircraft propulsion. The methodology is based on the well-known Euler equation which considers the change in angular momentum of the air as it passes through the fan rotors. A derivation of the useful and versatile Specific Work parameter (Y) is provided along with its important relationship with the fan Work Co-efficient (ψ) and an explanation of the relevance of the Fan Flow Co-efficient (ϕ) in determining the flow of air through the RDF device. An equation is derived which relates the fan torque to its rotational speed and a specimen calculation of a 200 mm inlet diameter RDF has been provided. Electrical performance graphs, generated with Motor-CAD LAB software, are included to illustrate an example of a suitably optimised RDF motor circuit. Finally, a thrust performance comparison is made between a theoretical dual-stage RDF and a commercially available fan-jet engine. It is demonstrated that the dual-stage RDF technology could offer a viable solution to power high-speed medium and large commercial transport aircraft, making them particularly suited to distributed thrust system architectures and blended-wing-body aircraft designs.**

Keywords—zero emission flight, rim driven fan, aircraft electrical propulsion, contra-rotating fans

I. Introduction

In the quest to achieve Zero Emission Flight (ZEF) by 2050 [1], Electrical Ducted Fans (EDFs) are increasingly being considered as a means of primary propulsion [2]. Most EDFs for aircraft propulsion are single-stage hub-driven devices that are powered using permanent magnet motor technologies. Rim Driven Fans (RDFs) [3]-[5], however, are a type of ducted fan that have a continuous rotor-rim attached to the tips of the fan blades and are driven by means of electro-magnetic motor circuitry arranged within the duct (Fig 1). RDFs offer some key advantages when compared with conventional hub-driven fans. Such as an increase in thrust per frontal area owing to the removal of the flow restriction caused by the hub-mounted motor; shorter overall length of the fan assembly; a reduction in the motor tangential forces required to generate torque owing to an increase in the radial moment arm; improved fan aerodynamics; provision of cooling for the motor windings and the ability to easily install two contra-rotating RDFs in tandem. This latter advantage also enables increased Fan Pressure Ratios (FPRs) to be generated [6] thus allowing faster efflux velocities and flying speeds. A drawback to an RDF configuration can be its weight if the electromagnetic circuit is not sized or constructed efficiently.

All fans have a finite limit to the amount of energy they can transfer to an air stream. This normally occurs when the fan operates under maximum static-thrust conditions and is governed by the tangential speed of the fan blades, the degree of air deflection (whirl) imparted by the blades and the mass flow rate of the air passing through the fan [7]. It is therefore important for the motor designer to estimate the required RDF torque versus speed characteristic, during the early stages of design, so that the electromagnetic motor circuit is not too powerful and heavy for its intended purpose. This is particularly relevant for the rim driven fan rotor which could otherwise become subject to unnecessary centrifugal loads.

II. Methodology

Euler's work equation defines the rate of transfer of angular momentum from a fan into the passing airstream and can be expressed as:

$$P = \dot{M} U \Delta C_W \qquad (1)$$

where, P is the fan shaft power (W); $\dot{M}$ is the mass flow of air passing through the fan, measured in kilograms per

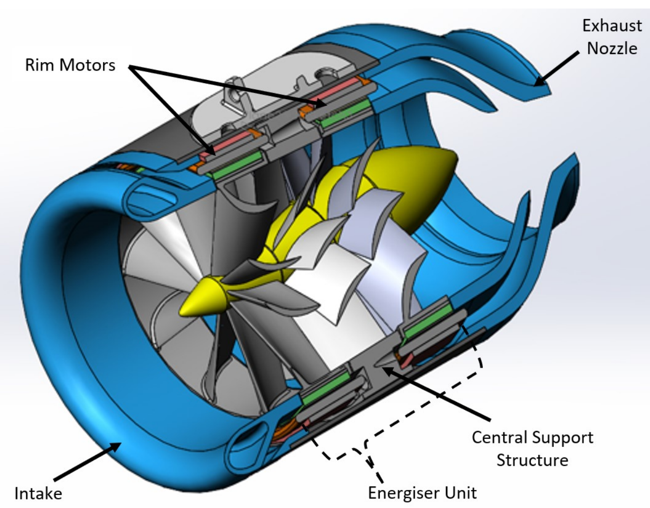

Fig. 1. Dual-stage RDF unit.

This work is funded by the Welsh Government (WEFO) under the SMARTExpertise initiative (Project Reference 82321) and is supported by the European Regional Development Fund.

second (kg/s); U is the tangential velocity of the fan (which is normally taken at a mean radius position) measured in metres per second (m/s); ΔC_W is the change in rotational (whirl) velocity of the airflow between the plane on which it enters the fan to that where it exits.

In equation (1) the term $U\Delta C_W$ defines the total specific work done by the fan and can be expressed in Joules per kilogram (J/kg). This term also represents the specific enthalpy rise of the air (Δh_0) and is widely given the symbol Y [8]. Total specific work Y is a very useful and versatile parameter in fan analyses and may be expressed in the following forms [6]:

$$Y = \frac{P}{\dot{M}} \tag{2}$$

$$Y = \frac{\Delta p}{\rho} \tag{3}$$

$$Y = U\Delta C_W \tag{4}$$

$$Y = C_p \Delta T \tag{5}$$

where, Δp is the total pressure rise across the fan (Pa); ρ is the average density of the air (kg/m^3), C_p is the specific heat capacity of air at constant pressure (taken as 1005 J/kg K); ΔT is the total temperature rise of the air across the fan (K).

To relate the specific work parameter (Y) to a particular fan device, for example, when considering the number, size, angles and shape of its blades etc., a dimensionless work co-efficient (also known as the Stage Loading) ψ is used [9], where:

$$\psi = \frac{\Delta C_W}{U} \tag{6}$$

Therefore, from equations (4) and (6) it can be determined that:

$$Y = \psi U^2 \tag{7}$$

Typical values of work co-efficient ψ for high-performance axial flow fans and compressors lie between $\psi = 0.4$ and $\psi = 0.75$ [9]. For radial (centrifugal) flow compressors, in which the airflow is turned through 90 degrees, a unity work co-efficient can be assumed i.e. $\psi = 1$.

To relate the tangential speed of the fan U to the axial velocity C_x of the airflow through the fan the dimensionless flow co-efficient, ϕ, is used, where:

$$\phi = \frac{C_x}{U} \tag{8}$$

An accepted value of flow co-efficient ϕ for high-performance axial flow fan and compressor designs is $\phi = 0.5$ [10].

The shaft power P of a fan is a product of the exerted torque T and the angular velocity of the fan ω and is expressed as follows:

$$P = T\omega \tag{9}$$

where, T is measured in Joules (J) or Newton metres (Nm); ω is the angular velocity of the fan measured in radians per second (rad/s).

The tangential velocity U can be determined from the angular velocity ω at any radial position of the fan using the following equation:

$$U = \omega r \tag{10}$$

where, r is the radial position (m).

Table I. Results of the Analysis of a 200 mm Intake Diameter Single-stage RDF using Equation (12).

Speed (RPM)	Speed (Rad/s)	Torque (Nm)
0	0.0	0.00
1000	104.7	0.03
2000	209.4	0.13
3000	314.1	0.29
4000	418.8	0.52
5000	523.5	0.81
6000	628.2	1.17
7000	732.9	1.60
8000	837.7	2.08
9000	942.4	2.64
10000	1047.1	3.26
11000	1151.8	3.94
12000	1256.5	4.69
13000	1361.2	5.50
14000	1465.9	6.38
15000	1570.6	7.33

From equations (2) and (7) the following relationship for shaft power can be derived:

$$P = \dot{M}\psi U^2 \tag{11}$$

From equations (8), (9), (10) and (11) the following relationship for shaft torque can be derived:

$$T = \omega^2 r_m^3 \phi \pi r_{in}^2 \rho \psi \tag{12}$$

where, r_m is the mean radial position (m), and r_{in} is the fan inlet radius (m).

III. Analyses and Results

A. *Estimating Torque versus Speed Characteristics of Electrically Powered Rim Driven Fans (RDFs)*

Table I and Fig. 2 show the results of the analysis of a 200 mm diameter single-stage RDF which were generated using equation (12). Assuming values of work co-efficient $\psi = 0.45$, flow co-efficient $\phi = 0.5$ and density $\rho = 1.225$ kg/m^3 i.e. International Standard Atmosphere (ISA) Sea Level conditions. An estimate for dual-stage RDF

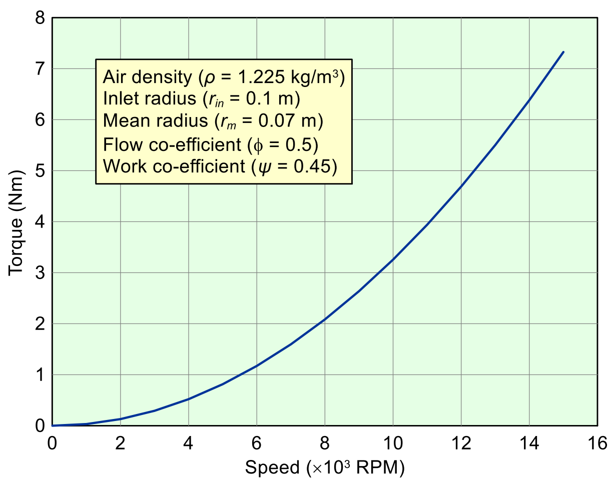

Fig. 2. Estimated Torque versus Speed Characteristic for a 200 mm diameter single-stage RDF.

TABLE II. RESULTS OF THE ANALYSIS OF A 600 MM INTAKE DIAMETER DUAL-STAGE CONTRA-ROTATING RDF.

Inlet diameter	0.6 m
Inlet radius	0.3 m
Mean radius	0.21 m
Speed	10000 RPM
Angular velocity	1047.07 Rad/s
Tangential velocity (U)	219.9 m/s
Work co-efficient (ψ)	0.45
Specific work (Y)	21757.04 J/kg
Flow co-efficient (ϕ)	0.5
Axial velocity (C_a)	109.9 m/s
Hub diameter	0.05 m
Inlet area	0.275 m^2
Volume flow	30.218 m^3/s
Mass flow	37.017 kg/s
Dual RDF (Y dual)	43514.08 J/kg
Δp	53304.7 Pa
Fan Pressure Ratio (FPR)	1.526
Efflux velocity	295 m/s
Shaft Power	1.6108 MW
Torque	1538.4 Nm
Torque (single)	769.2 Nm
Thrust Static	10920.3 N
Thrust Static	1113.2 kg
Thrust Static	2493.5 lb

performance can be made by doubling the Specific Work (Y) value calculated for a single-stage RDF.

Fig. 2 shows that there is a gradual but exponential increase in the shaft torque requirement with respect to increasing fan speed. This curve is typical of torque versus speed characteristics for pumps, fans, ship propulsion etc. [11].

B. Matching RDF Motor Performance to the Torque versus Speed Characteristics

Using the results provided in Table I and Fig. 2 it was possible to match the design of the rim motor to satisfy the maximum fan torque requirement (7.33 Nm at 15,000 RPM) so that the RDF was neither overpowered nor overweight. Figs. 3-5 show graphs created using MotorCAD LAB software [12], of shaft torque, shaft power, and motor efficiency versus motor speed. These graphs were generated based on a novel AC synchronous rim motor arrangement designed to drive a single 200 mm diameter fan. The details of the actual motor are commercially sensitive. However, the reduced tangential rim forces meant that a very lightweight motor design was achieved. The motor has an iron-less rotor design based on a Halbach-array of permanent magnets and an optimised multi-slotted, thin laminated stator iron with aluminium, 3-phase distributed windings and flux densities not exceeding 1.2 Tesla. An increased voltage supply also enabled a lower operating current (peak value = 35 A) compared with an equivalently rated hub-driven EDF that normally draws more than 200 A. The reduced RDF current also minimises the heating losses in both the motor and the controller, and Fig. 5 shows the

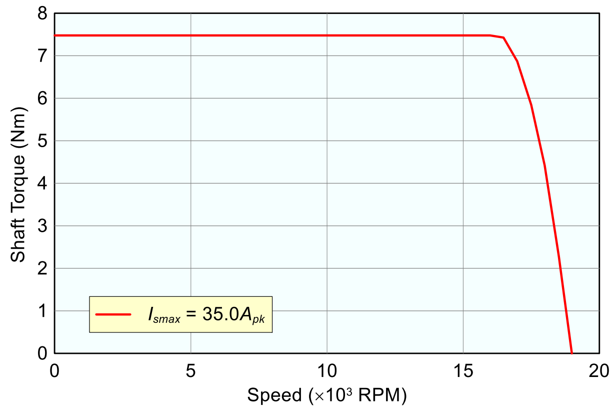

Fig. 3. Shaft torque versus speed characteristic for a 200 mm diameter fan single stage RDF motor, Motor CAD (LAB).

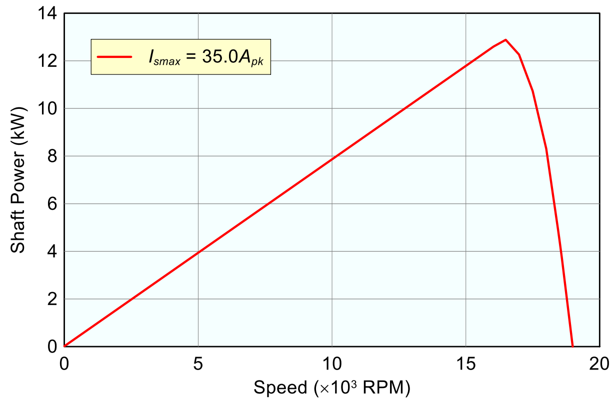

Fig. 4. Shaft power versus speed characteristic for a 200 mm diameter fan single stage RDF motor, Motor CAD (LAB).

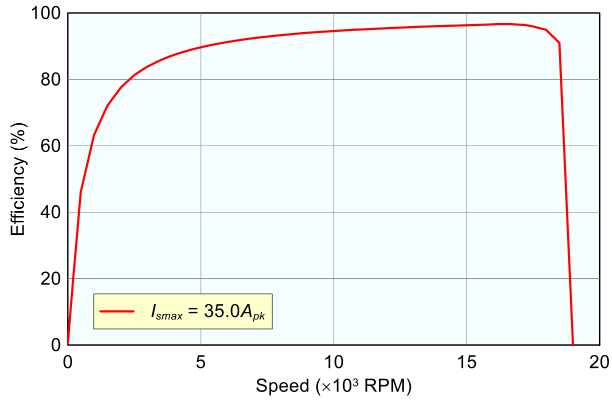

Fig. 5. Efficiency versus speed characteristic for a 200 mm diameter fan single stage RDF motor, Motor CAD (LAB).

Fig. 6. Pratt and Whitney PW617F-E Engine [15].

Table III. Comparison between the Physical Dimensions and Static Thrust Values for the PW617F-E Engine.

Parameter/ Engine	**PW617F-E**	**Dual Stage RDF Energiser**
Static Thrust (lb)/(N)	2,050/8,978	2,494/10,920
Fan diameter (mm)	447	600
Engine Length (mm)	1,257	510

Fig. 7. UK MOD Phenom T1 Training aircraft [16].

high motor efficiency of approximately 95% that is achieved at 15,000 RPM. This optimised RDF motor design resulted in a Specific Power rating of approximately 4 kW/kg when accounting its active elements [13],[14].

C. Comparison of a Dual Stage Electrical RDF and a Conventional Fan Jet Engine

Using the equations established in the Methodology section, a comparison has been made between the theoretical thrust performance of a 600 mm diameter dual-stage contra-rotating RDF energiser unit (Fig. 1) with an existing small fan-jet engine, namely the Pratt and Whitney W617F-E, used to power the UK's Royal Air Force Phenom -T1 aircraft (Figs. 6 and 7). The RDF calculations estimate its performance whilst it is operating at maximum static thrust, at 10,000 RPM under ISA Sea Level conditions. Refer to Table II for the input data and calculated results.

Fig. 8. AERALIS Basic Jet Trainer concept aircraft [17].

Fig. 9. Airbus ZEROe BWB, distributed thrust concept aircraft [18].

Table II indicates the potential for RDF technology to power high-speed aircraft in place of current turbojet and fan-jet engines. The estimated maximum efflux velocity of this dual RDF example is 295 m/s (660 mph) and the static thrust is 10.92 kN (2494 lbs). This device could be used to power a light military trainer aircraft (Fig. 8) or alternatively a multitude of RDF devices could power medium to large commercial aircraft configured with BWB distributed thrust systems (Fig. 9).

Table III provides a basic comparison between the PW617F-E engine [15],[19] and a dual-stage electrical RDF. The RDF diameter is 34% larger than the PW617F-E, although it is 60% shorter in length. The RDF also provides a much higher thrust capability (10.92 kN) compared to the PW617F-E (8.98 kN).

IV. Conclusion

Equation (12) has been derived, which can be used for estimating torque versus speed characteristics of single and dual-stage electrically powered Rim Driven Fans (RDFs) intended for aircraft propulsion. This can assist the aeronautical motor designer to optimise the electromagnetic circuit and minimise the motor's mass and centrifugal stresses. The calculated values of shaft torque and rotational speed can also be used to determine the required motor shaft power and, by assuming values for motor and controller efficiencies, estimate the electrical power supply requirements. An example of an optimised RDF motor has also been provided using MotorCAD generated torque, power and efficiency characteristics. This optimised RDF motor design resulted in a Specific Power rating of approximately 4kW/kg which is comparable to state-of-the-art hub driven EDF devices.

The results of the comparative study between the theoretical dual-stage RDF and the Pratt and Whitney PW617F-E fan-jet engine indicated that, as a thruster device, the RDF offers a compact and lightweight alternative to small fan-jet engines. The RDF is also substantially shorter in length, will operate at much lower core temperatures than a jet engine and is likely to be lighter in weight, more efficient, easier to monitor and control, quieter and offer much greater values of specific thrust. It is considered that the only reason why RDFs are not already used for ZEF, on pure electric aircraft, is because of existing technology limitations regarding on-board electrical energy storage and delivery. However, RDFs are a viable contender for high-speed hybrid aviation applications such as large BWB commercial aircraft with distributed thrust architectures that are being studied by Airbus [18] and NASA [20].

References

[1] United Nations Framework Convention on Climate Change. (2015, December 12). Paris Agreement: FCCC/CP/2015/L.9/Rev.1. [Online]. Available: https://unfccc.int/resource/docs/2015/cop21/eng/l09r01.pdf

[2] R.C. Bolam, Y. Vagapov, and A. Anuchin, "Review of electrically powered propulsion for aircraft," in *Proc. 53rd Int. Universities Power Engineering Conf.*, Glasgow, UK, 4-7 Sept. 2018, pp. 1-6, doi: 10.1109/UPEC.2018.8541945

[3] R.C. Bolam, Y. Vagapov, R.J. Day, and A. Anuchin, "Aerodynamic analysis and design of a rim driven fan for fast flight," *Journal of Propulsion and Power*, vol. 37, no. 2, pp. 179-191, March 2021, doi: 10.2514/1.B37736

[4] H. Yang, Y. Wang, J. Sun, B. Wang, Y. He, and P. Song, "Design and flow analysis of a rim-driven hub-less axial flow fan," in *Proc. ASME Turbo Expo: Turbomachinery Technical Conference and Exposition*, Online, 7-11 June, 2021, vol. 2A, pp. 1-9, doi: 10.1115/ GT2021-58812

[5] R.C. Bolam, and Y. Vagapov, "Implementation of electrical rim driven fan technology to small unmanned aircraft," in *Proc. 7th Int. Conf. on Internet Technologies and Applications ITA-17*, Wrexham, UK, 12-15 Sept. 2017, pp. 35-40, doi: 10.1109/ ITECHA.2017.8101907

[6] R.C. Bolam, Y. Vagapov, J. Laughton, and A. Anuchin, "Optimum performance determination of single-stage and dual-stage (contra-rotating) rim-driven fans for electrical aircraft," in *Proc. XI Int. Conf. on Electrical Power Drive Systems*, St. Petersburg, Russia, 4-7 Oct. 2020, pp. 1-6, doi: 10.1109/ICEPDS47235.2020.9249263

[7] H.I.H. Saravanamuttoo, G.F.C. Rogers, H. Cohen, P.V. Straznicky, and A. Nix, *Gas Turbine Theory*, 7th ed. Harlow: Pearson Prentice Hall, 2017.

[8] W. Bohl, *Ventilatoren: Berechnung, Konstruktion, Versuch, Betrieb*. Wurzburg: Vogel, 1083.

[9] S.L. Dixon, and C.A. Hall, *Fluid Mechanics and Thermodynamics of Turbomachinery*, 7th Edn. Amsterdam: Butterworth-Heinemann, 2014.

[10] R.H. Aungier, *Axial Flow Compressors: A Strategy for Aerodynamic Design and Analysis*. New York: ASME Press, 2003.

[11] G. Abad, *Power Electronics and Electric Drives for Traction Applications*. Chichester: Wiley, 2017

[12] J. Goss, "Performance analysis of electric motor technologies for an electric vehicle powertrain," Wrexham, UK, Motor Design Ltd., White Paper, 2019. [Online]. Available: https://www.motor-design.com/wp-content/uploads/2019/06/Performance-Analysis-of-Electric-Motor-Technologies-for-an-Electric-Vehicle-Powertrain.pdf

[13] R.C. Bolam, Y. Vagapov, and A. Anuchin, "A review of electrical motor topologies for aircraft propulsion," in *Proc. 55th Int. Universities Power Engineering Conf.*, Torino, Italy, 1-4 Sept. 2020, pp. 1-6, doi: 10.1109/UPEC49904.2020.9209783

[14] M. Rosu, P. Zhou, D. Lin, D. Lonol, M. Popescu, F. Blaabjerg, V. Rallabandi, and D. Staton, *Multiphysics Simulation by Design for Electrical Machines, Power Electronics and Drives*. Piscataway, NJ: IEEE Press; Hoboken, NJ: Wiley, 2018.

[15] Pratt & Whitney [Online]. Available: https://www.pwc.ca/en/products -and-services

[16] Royal Air Force. Phenom-T1. [Online]. Available: https:// www.raf.mod.uk/aircraft/phenom-t1

[17] Arealis. [Online]. Available: https://aeralis.com

[18] Airbus. (2020, September 21). Airbus reveals new zero-emission concept aircraft [Online]. Available: https://www.airbus.com/sites/g/ files/jlcbta136/files/d82a792c20d166f4700d20c013fead8a_EN-Airbus-unveils-ZEA-concepts.pdf

[19] EASA. (2017, May 19). Type-Certificate Data Sheet No. IM.E.125 [Online]. Available: https://www.caa.co.uk/Documents/ Download/3939/984aa08e-5352-4da9-824b-309ec7cec37d/3032

[20] NASA. (2013, February 14). Hybrid wing body goes hybrid. [Online]. Available: https://www.nasa.gov/content/hybrid-wing-body-goes-hybrid